Polyphenol oxidase inactivation from apple juice by Al-based metal–organic frameworks: New anti-browning strategy in fruits and vegetables

Norma A. Marrufo-Hernández [a], Hugo Nájera [b], Fernando González Chávez [c], Hiram I. Beltrán [d]

[a] Posgrado en Ciencias Naturales e Ingeniería, Universidad Autónoma Metropolitana, Unidad Cuajimalpa, Av. Vasco de Quiroga 4871, Col. Santa Fe Cuajimalpa, Cuajimalpa de Morelos 05348, CDMX, Mexico
[b] Departamento de Ciencias Naturales, DCNI, Universidad Autónoma Metropolitana, Unidad Cuajimalpa, Av. Vasco de Quiroga 4871, Col. Santa Fe Cuajimalpa, Cuajimalpa de Morelos 05348, CDMX, Mexico
[c] Universidad Politécnica del Estado de Nayarit, Calle Dr. Ignacio Cuesta Barrera S/N Carretera Tepic-Aguamilpa Ejido la Cantera, 63506 Tepic, Nayarit, Mexico
[d] Departamento de Ciencias Básicas, DCBI, Universidad Autónoma Metropolitana, Unidad Azcapotzalco, Av. San Pablo No. 180, Col. Reynosa Tamaulipas, Azcapotzalco 02200, CDMX, Mexico

ARTICLE INFO

ABSTRACT

Polyphenol oxidase (PPO) is critical due to enzymatic browning in fruits and vegetables, developing economic impact in fruits industry. Metal-Organic Frameworks (MOF) have shown interesting characteristics such as water stability, low toxicity, and good adsorption yield, making them good candidates for PPO inactivation. Al-based-MOFs, MIL-53(Al), DUT-5, and MIL-110 were tested as PPO inactivators in apple juice by enzyme-MOF interactions at r.t. through two possible mechanisms, i) substrate scavengers (substrates:catechol and 4-methylcatechol) or ii) enzyme activity modifiers. The scavenging behavior of Al-based-MOFs was moderate, in the same magnitude, being catechol adsorption better than 4-methylcatechol. PPO activity was reduced by at least 70% by MIL-53(Al)/DUT-5 in 10/30 min respectively, and MIL-110 inactivated PPO in 50 min with some structural modifications. Enzyme-MOF interactions are major responsible for PPO inactivation. This could be a new applicability of MOFs, as an alternate PPO inactivation process, easily included in juice processing, retaining sensorial/nutritional properties, developed at r.t thus energy-cost-effective.

1. Introduction

Polyphenol oxidases (PPO) are a group of metalloenzymes with copper in their active site, they are widely distributed in animals, plants, fungi, and bacteria (Mayer, 2006; Queiroz, Mendes Lopes, Fialho, & Valente-Mesquita, 2008). PPO is known for the catalysis of polyphenol oxidation that finally produces melanoid compounds, which give undesirable dark colors, flavors, and odors as well as losses in nutrients and general quality in foods, this is commonly known as fruits and vegetables enzymatic browning (Queiroz et al., 2008). Due to this and the great impact that this browning has on producers and the food industry, the PPO has been widely studied to develop new and better inactivation methodologies, precisely to mitigate or preferably inhibit this browning (Mayer, 2006; Queiroz et al., 2008; Yoruk & Marshall, 2003).

Thermal inactivation was studied for a wide variety of fruits, with variations in time/temperature from 60 to 90 °C and between <2–15 min (Ni Eidhin, Murphy, & O'Beirne, 2006; Terefe, Delon, Buckow, & Versteeg, 2015) where standardized inactivation for all PPO is not possible. On the other hand, the use of chemical compounds, for example, reducing agents, acidic, and chelating-complexing agents, represents other alternatives to achieve inhibition/inactivation (Yoruk & Marshall, 2003). To name a few disulfide (Ni Eidhin et al., 2006; Palma-Orozco, Marrufo-Hernandez, Sampedro, & Najera, 2014; Palma-Orozco, Ortiz-Moreno, Dorantes-Alvarez, Sampedro, & Najera, 2011), and cysteine (Janovitz-Klapp, Richard, & Nicolas, 1989; Liu, Zhao, Gan, & Ni, 2015), have been able to inhibit PPO, nevertheless in some others, the effectiveness is variable and/or regulated or prohibited owe to their negative effects in human health (Yoruk & Marshall, 2003). Also, alternative technologies like microwaves (Palma-Orozco, Marrufo-Hernández, Tobías, & Nájera, 2019; Palma-Orozco et al., 2011), high-pressure (Terefe et al., 2015), high-humidity air impingement blanching (Bai, Gao, Xiao, Wang, & Zhang, 2013), ohmic heating (Makroo,

Saxena, Rastogi, & Srivastava, 2017), ultrasound (Palma-Orozco et al., 2019), manothermosonication (Lopez, Sala, de la Fuente, Condon, Raso, & Burgos, 1994), and cold plasma (Illera et al., 2019) have been tested. Some were reported as good PPO inhibitors/inactivators, meanwhile, others need to be combined with high temperatures or chemical compounds to reach the inhibition/inactivation (Palma-Orozco et al., 2011). Some others were related to losses in nutritional content and changes in the sensorial properties (Devece et al., 1999; Fu, Zhang, Wang, & Du, 2007), where PPO inactivation continues to be an attractive field of research aiming for price diminishment, as well as yield, nutritional and sensorial quality enhancement (Iqbal, Murtaza, Hu, Ahmad, Ahmed, & Xu, 2019; Queiroz et al., 2008).

Besides, Metal-Organic Frameworks (MOF) are one of the most studied materials, being a promising field of research in chemistry and materials science (Eddaoudi, Sava, Eubank, Adil, & Guillerm, 2015), due to their versatility and potentiality for a wide variety of applications (Gkaniatsou, Sicard, Ricoux, Mahy, Steunou, & Serre, 2017), included aqueous solutions and food (Barreto et al., 2010; Patil, Rallapalli, Dangi, Tayade, Somani, & Bajaj, 2011; Qian et al., 2013). MOFs are crystalline and porous networks of metallic nodes and organic linkers (Gkaniatsou et al., 2017) that have interesting qualities like the surface area between 100–7000 $m^2 \cdot g^{-1}$, porosity >90% of free volume, and wide versatility existing infinite metals-linkers combinations (Eddaoudi et al., 2015). Additionally, some of them have shown water stability, biodegradability, biocompatibility (Grall, Hidalgo, Delic, Garcia-Marquez, Chevillard, & Horcajada, 2015; Singh, Qutub, & Khashab, 2021), as well as tunable toxicity (Ettlinger et al., 2022; Wiśniewska, Haponiuk, Saeb, Rabiee, & Bencherif, 2023). All of this has turned them very attractive for industrial (Kong & Li, 2021), environmental (Liang et al., 2020; Zhang, Yang, Zhou, Chen, Li, & Pang, 2022), or agricultural usage (Rojas, Rodriguez-Dieguez, & Horcajada, 2022), where certain groups have highlighted unaddressed challenges and provided some important directions for future basic and applied research (Liang et al., 2020; Majewski, Noh, Islamoglu, & Farha, 2018; Steenhaut, Filinchuk, & Hermans, 2021). Some of the more recent highlights are their potential as biomimetic mineralization agents, as smart biostimulant delivery systems, and crop micronutrients fortifiers, turning them into good candidates to be applied in food processes and food applications (Aguliar Perez et al., 2023; Barreto et al., 2010; Fu et al., 2023; Patil et al., 2011; Pinar Gumus & Soylak, 2021; Richardson & Liang, 2018; Sierra-Serrano et al., 2022; Wu, Du, Ma, Shen, & Zhou, 2019).

In particular, Al-based-MOFs have proven to develop many very good physicochemical characteristics, chemical/structural stability at high temperatures, and in contact with organic solvents, water, and air, besides they present versatility or tuneability in their chemical structures (Fan et al., 2023; Samokhvalov, 2018). These materials have shown very high capacities and selectivities, aimed for molecular or even ionic sorption/separations, as heterogeneous catalysts, as well as in sensing applications (Samokhvalov, 2018). Another very important set of characteristics is related to the contact/interaction of these Al-based-MOFs with biosystems, therefore their water stability (Samokhvalov, 2018), biodegradability, biocompatibility, and low toxicity, even in comparison with Fe-based-MOFs, has been underlined very recently (Fan et al., 2023). Just to finally emphasize that aluminum is considered a non-toxic metal, it is also quite inexpensive, and unexpectedly it resulted more abundant than Fe or Ca on Earth's crust, therefore suitable to be applied in a myriad of fields (Fan et al., 2023).

Despite this, there are a few studies in the food field with MOFs (Kong & Li, 2021) for example these materials have been tested for the removal (Barreto et al., 2010; Liu et al., 2016) or as smart delivery systems (Xu, Cao, Liu, Chen, & Li, 2023) of pesticides, herbicides, lead, insecticides (extraction and controlled release) (Chauhan, Omar, Mangalaraja, Ashfaq, & Talreja, 2022), endocrine disrupting compounds, phthalate esters, and benzoylurea. All this research reported that MOFs have good selectivity and adsorption of problematic compounds as well as better yield related to conventional methodologies (Islamoglu et al., 2020).

The group of MOF synthesized in the Materials Institute Lavoisier called (MIL)-53(M) (M = Fe/Al/Cr) has shown interesting properties, for example, MIL-53(Al) presented water stability in high temperatures (<100 °C) using acidic or neutral conditions (Qian et al., 2013), good extraction of polycyclic aromatic hydrocarbons (Chen et al., 2012), and immobilization of some proteins such as trypsin, hemoglobin, laccase, glucose oxidase, among others (Gkaniatsou et al., 2017).

Therefore, we propose/hypothesize to use MOFs, especially water-stable materials like MIL-53(Al), DUT-5, and MIL-110 as PPO inactivators, which could result in a promising/innovative alternative for juice processing/conditioning, and this process could be carried out at room temperature to minimize industrial expenses.

2. Methodology

2.1. General information

Golden delicious (GD) apples were from Chihuahua, Mexico, and ripened for four weeks at room temperature. Apple Juice was extracted from peeled and seedless apples with a Turmix juice extractor, filtered, and centrifuged at 7,200 *g* for 15 min (Genovese, Elustondo, & Lozano, 1997). 1,3,5-benzenetricarboxylic (trimesic, BTC) and 4, 4′-biphenyldicarboxylic (BDCA), and benzene-1,4-dicarboxylic (BDC) acids were purchased from TCI America, ammonium sulfate, N,*N*-dimethylformamide (DMF) and methanol (MeOH) from JT Baker and the rest of chemical compounds were purchased from Sigma-Aldrich, St. Louis, MO, USA. Plots and data analysis were made with Origin 8.0 software.

2.2. Synthesis and characterization of water-stable Al-based-MOFs

2.2.1. Synthesis of MIL-53(Al)

MIL-53(Al) was synthesized from 1.3 g (3.46 mmol) of Al $(NO_3)_3 \cdot 9H_2O$, 0.28 g (1.73 mmol) of BDC, and 20 mL of deionized water, all this was mixed in a 45 mL Teflon® cell, placed and sealed inside a stainless steel reactor, and finally heated 3 days at 220 °C (Loiseau et al., 2004). The white precipitate obtained was vacuum-filtered, washed with deionized water (4 × 50 mL), and left overnight in 25 mL of DMF. The material was vacuum filtered and washed with hot DMF (2 × 20 mL), the filtrate was vacuum dried and left 2 h in 25 mL of MeOH, removing occluded DMF (Rallapalli, Patil, Prasanth, Somani, Jasra, & Bajaj, 2010), and the solid was dried 4 h at 150 °C, yielding 60% of MIL-53(Al).

2.2.2. Synthesis of DUT-5

DUT-5 was prepared from a slightly modified procedure (Gotthardt et al., 2015). A solution of 1 g (4.12 mmol) of BDCA in 100 mL of DMF was prepared by 15 min of ultrasound treatment at 750 kHz frequency, 40% power (Ultrasound equipment, brand Sonics, model High-Tech Processor-750). Another solution of 2.32 g (6.18 mmol) of Al $(NO_3)_3 \cdot 9H_2O$ in 25 mL of DMF was prepared by stirring at room temperature reaching dissolution. To start the reaction, 20 mL of BDCA-solution was poured into a two-necked flask and 5 mL of Al-solution was slowly added while the mixture was stirring, this mixture was carried to reflux (≈130 °C) until a white precipitate was observed. To enhance the crystal growth of this MOF, the initial solutions were added in five parts as follows, 20 mL of BDCA-solution followed by 5 mL of Al-solution were added to the reaction flask each 20 min until they were finished, and the total mixture was left in reflux 24 h. The white precipitate obtained was vacuum filtered and washed with DMF (4 × 50 mL). DUT-5 was washed for 15 min with DMF (3 × 50 mL) by ultrasound treatment (same conditions as stated above), and the product was dried for 8 h at 200 °C yielding 56% of DUT-5.

2.2.3. Synthesis of MIL-110

MIL-110 was synthesized by 0.6 g (2.4 mmol) BTC, 1.34 g (3.6 mmol)

of Al(NO)$_3$·9H$_2$O, 0.53 mL of nitric acid (65%), and 10 mL of deionized water, all mixed in a 45 mL Teflon cell, placed and sealed inside a stainless steel reactor for 3 days at 220 °C. The white precipitate obtained was washed with deionized water (4 × 50 mL), and dried for 8 h at 150 °C, yielding 57% of MIL-110 (Haouas, Volkringer, Loiseau, Férey, & Taulelle, 2012).

2.2.4. Adsorbent water-stable aluminum-based MOFs conditioning

The synthesized MIL-53, DUT-5, MIL-110, and activated carbon (AC, as a reference juice clarifying material, CODEX STAN 247–2005) ("Norma general del CODEX para zumos (jugos) y néctares de frutas (CODEX STAN 247-2005)," 2005), were washed 24 h stirring at room temperature with 100 mL of deionized water. Followed by vacuum filtration with a Durapore membrane (0.45 μm, polyvinylidene fluoride, HVLP04700), dried for 8 h at 130 °C. To corroborate the removal of occluded reagents into the materials, UV–Vis spectroscopy was recorded (λ = 200–900 nm) obtaining flat spectra.

2.2.5. Al-based-MOFs adsorption with reference PPO substrates

Adsorption experiments between Al-based-MOFs with aqueous solutions of catechol (Cat) or 4-methyl-catechol (4-MC) were carried out to test PPO-inactivation mechanism by substrate scavenging (Mayer, 2006), banning substrate availability for PPO oxidation. Tests employed 20 mg of each, MIL-53(Al), DUT-5, MIL-110, and AC, adsorbent that were added to 40 mL of each 5 mM substrate solution, this was reported as the maximum concentration of polyphenols for GD apples from some countries including Mexico (Núñez-Gastélum, Alvarez-Parrilla, de la Rosa, Martínez-Ruíz, González-Aguilar, & Rodrigo-García, 2015). Both components, MOFs, and substrates, interacted for 30 min at 200 rpm stirring. Samples of 2 mL of each experiment were taken at 1, 5, 10, 20, and 30 min, and filtrated with Durapore membrane, the filtered solutions were measured by UV–Vis (λ$_{min}$ = 250 nm) for substrate quantification using a calibration curve (Marrufo-Hernández, Palma-Orozco, Beltrán, & Nájera, 2017; Palma-Orozco et al., 2019).

2.3. Apple juice PPO inactivation with Al-based-MOFs

2.3.1. Adsorption and inactivation of PPO in apple juice

The prepared apple juice, 40 mL, was mixed with 20 mg of each material (MIL-53(Al), DUT-5, MIL-110, and AC) interacting for 50 min, by stirring at 200 rpm. Samples of each experiment were taken at 1, 10, 20, 30, and 50 min, materials were removed by filtration with a Durapore membrane and characterized as follows.

2.3.1.1. PPO activity.
PPO activity was determined at 25 °C through an Agilent 8453 UV–Vis (New York, USA) diode array spectrophotometer. Reaction medium, 1 mL, at 50 mM catechol in 0.2 M sodium phosphate buffer pH 7.0 was used, and 33 μL of samples were added to start the reaction, monitored through ΔAbs$_{420nm}$ every 15 s, during 5 min. The change in the absorbance of 0.001·(min·mg)$^{-1}$ of the enzyme was defined as one unity of PPO activity. The activity of centrifuged and filtrated juice without adsorbent interaction was set as 100% of the activity (Marrufo-Hernández et al., 2017; Palma-Orozco et al., 2019).

2.3.1.2. Protein quantification.
Samples were diluted 1:10 with deionized water and protein concentration was determined by UV–vis at λ$_{280nm}$ (Walker, 2009) using a correlation factor for plants of 0.8 (Bollag, Rozycki, & Edelstein, 1996).

2.3.1.3. Physicochemical characterization.
The density, pH, and soluble solids content of samples were measured according to NMX-F-045-1982 ("NMX-F-045-1982. Alimentos frutas y derivados, Jugo de manzana. Foods, Fruits and derivatives, apple juice normas mexicanas.," 1982). The pH was measured with a HANNA-HI98130 multiparameter device. Sugar content and refractive index (RI) were measured in 0.1 mL of juice

with an ATAGO Abbe NAR-1 T LIQUID refractometer, all measurements were made by triplicate prior to or after filtration.

2.3.2. Al-based-MOFs characterization after interaction with substrates or juice

The adsorbent materials, X = MIL-53(Al), DUT-5, MIL-110, and AC, were characterized and labeled as synthesized (X), after conditioning (X-C), after adsorption test with catechol (X-Cat), with 4-methylcatechol (X-4-MC), and with juice (X-J). FTIR spectra were obtained from solid diluted samples with KBr in a Bruker Tensor-27 spectrophotometer by specular reflectance, in 4000–450 cm^{-1}. The powder X-ray diffraction (PXRD) patterns were obtained in a Bruker D2-Phaser diffractometer with a coupled copper anode X-ray radiation (Cu K$_\alpha$1, λ = 1.5406 Å), 0.2°·s^{-1} scanning speed, in 2θ from 6 to 35°. Scanning electron microscopy (SEM) images were obtained with a microscope Hitachi-TM3030PLUS at 15 kV with Back-scattered electrons.

3. Results and discussion

This work aimed to survey GD apple PPO inactivation employing water-stable and low toxicity Al-based-MOFs materials, in this case, MIL-53(Al), DUT-5, and MIL-110. This could be achieved by different pathways, being MOFs (i) substrate scavengers or (ii) enzyme activity modifiers. The corresponding results will be discussed as follows.

3.1. Adsorption with PPO reference substrates

Al-based-MOFs and AC were tested as adsorbents with PPO substrates, catechol, and 4-MC, at 5 mM (highest polyphenol concentration reported in apples), to test if the Al-based-MOFs behave as substrate scavengers. If this is the mechanism, substrates will rarely be available to interact with PPO. Fig. 1 evidences that all materials are capable of adsorbing the reference substrates (type I patterns), except for DUT-5 with catechol that presented a type IV isotherm (Thommes et al., 2015). AC reaches its maximum adsorption at short times and then tends to release < 5 % of the adsorbed substrate. Contrastingly, the Al-based-MOFs slowly saturated, reaching their maximums at *ca.* 30 min. The best for catechol was DUT-5 adsorbing 180.9 mg·g^{-1}, and for 4-MC was AC with 372.1 mg·g^{-1}, this latter denoting a higher selectivity for the less polar substrate. Al-based-MOFs selectively adsorbed the more polar substrate, with the exception of MIL-53(Al). Nevertheless, the maximum adsorption into Al-based-MOFs reached, at most, 16% of the total available substrates, therefore this mechanism should not be playing a major role in PPO inactivation.

Variable molecular adsorption times or concentrations have been reported for many MOFs in aqueous solution, e.g. maximum adsorption, 625 mg·g^{-1}, below 20 min has been reported for nitrobenzene [≈2 mM] with MIL-53(Al) (Patil et al., 2011), for methylene blue and methyl violet with Cu-terephthalate-Fe$_3$O$_4$-nanorods maximum adsorption <5 min, *ca.* [3.74 mg·L^{-1}] (Li, Yuan, Hong, Fan, Mao, & Liu, 2015). The equilibrium times for the removal of bisphenol (Qin, Jia, Liu, Li, & Wu, 2015)/malachite green (Huo & Yan, 2012) with MIL-100(Fe) [55.6/250.0 mg·g^{-1}], MIL-101(Cr) [252.5/75 mg·g^{-1}], AC [137.0/150 mg·g^{-1}], and just for the latter MIL-53(Al) [50 mg·g^{-1}] were reached at t < 60 min or 60 h respectively. Adsorption of diclofenac disodium salt from aqueous media with UiO-66(Zr) [189 mg·g^{-1}], and AC [76 mg·g^{-1}] occurred at t > 12 h to reach equilibrium (Hasan, Khan, & Jhung, 2016). This analysis allowed stating that the Al-based-MOFs used herein have shown sharp adsorption times with catechol and 4-MC.

Particularly, Al-based-MOFs MIL-53(Al)–NH$_2$, MIL-68(Al), MIL-100 (Al), MIL-101(Al), and MIL-101(Al)–NH$_2$, were tested to adsorb [mg·g^{-1}] methylene blue (MB), malachite green (MG) and methyl orange (MO) as cationic and anionic dyes from aqueous solutions. MIL-53 (Al)–NH$_2$ adsorbed 188.6 of MB and 152.1 of MG; in contrast, MIL-68 (Al) adsorbed 666.7 of MB, 153.85 of MG, and 188.0 of MO; for the MIL-100(Al) was just tested with MO, adsorbing 265.0; the MIL-101(Al)
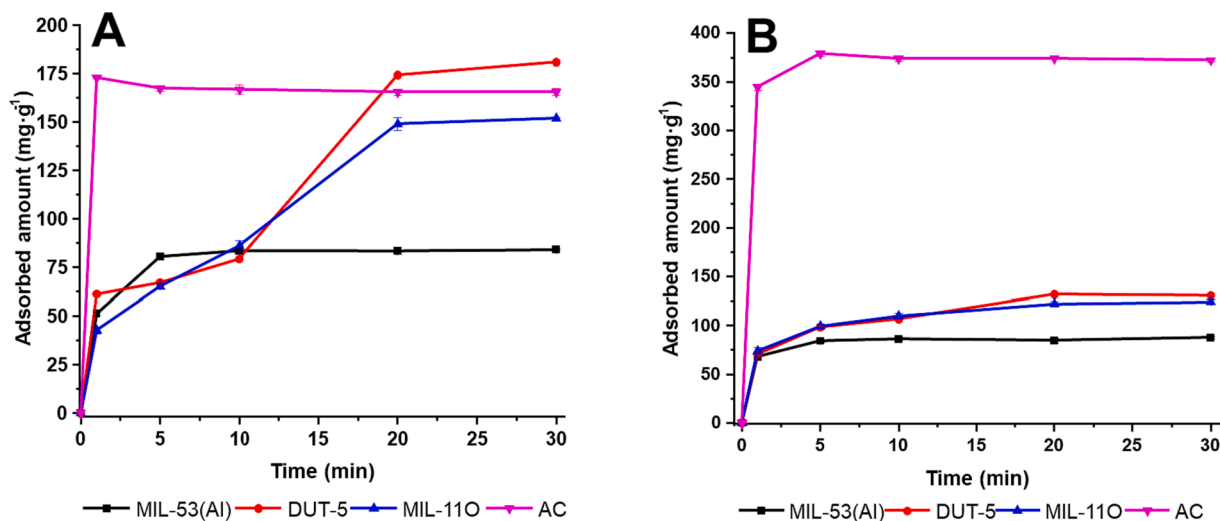
Fig. 1. Adsorption kinetics of Al-based-MOFs and AC for A) Catechol and B) 4-MC at 5 mM in t = 0–30 min (means of three replicates with standard deviation <5 %).

was only tested with MB and adsorbed 195.0; finally MIL-101(Al)–NH$_2$ adsorbed 162.0 of MB, and 265 of MOF (Haque, Lo, Minett, Harris, & Church, 2014; Samokhvalov, 2018).

According to the latter, the adsorbing capacity of tested materials against those described in the literature is among the same magnitude, with slight differences depending on the host(MOF)/guest(molecule) affinity. E.g. MIL-53(Al) adsorption varies considerably with nitrobenzene (625 mg·g^{-1}) (Patil et al., 2011), malachite green (50 mg·g^{-1}) (Huo & Yan, 2012), catechol (85 mg·g^{-1}), and 4-methylcatechol (83 mg·g^{-1}), where adsorption capacity of this material enhances as the size of the molecule diminishes and the polarity increases (Qin et al., 2015).

3.1.1. Juice adsorption

To analyze if the materials are capable of adsorbing/interacting with proteins, and achieving PPO inhibition, the adsorbent capacity of MIL-53(Al), DUT-5, MIL-110, and AC was determined. Fig. 2A depicts the apple juice PPO inhibition profiles of tested materials, for AC the PPO activity remained at t < 20 min, and became hyperactive after t = 20 min, reaching 140%. Besides, DUT-5 reached the lowest activity at 10 min (30%), gradually recovering achieving 130% at t = 50 min. Similar behavior was observed for MIL-53(Al) (Loiseau et al., 2004), probably due to the structural similarity of this MOF against DUT-5 (Senkovska,

Hoffmann, Fröba, Getzschmann, Böhlmann, & Kaskel, 2009), reaching a minimum of 30% at t = 30 min, recovering to a lower degree (50%) at t = 50 min.

On the other hand, MIL-110 which is structurally different from DUT-5 and MIL-53(Al) was the only one capable of inactivating PPO, also the inactivation kinetics is different from the other materials (Fig. 2A), where PPO activity diminishes reaching 3% at t = 30 min and inactivating at t = 50 min. Finally, the apple juice PPO control (green curve) remained ca. 100%. Hence the (hyper/in) activation effect could be attributed to PPO/materials interaction.

To the best of our knowledge, there were not found research contributions with PPO-MOF composites. Nevertheless, MOFs have served as stabilizing agents, encapsulating/immobilizing a great variety of enzymes/proteins for different purposes, researching the stabilization mechanisms, like i) surface adsorption based on electrostatic/hydrophobic interactions, and van der Waals forces (Gkaniatsou et al., 2017), ii) covalent bonding between free functional groups in MOFs and proteins (Gkaniatsou et al., 2017), and iii) encapsulation, where relative small size proteins diffuse through the cavities to the interior of the MOF material (Gkaniatsou et al., 2017). Microperoxidase-11 was immobilized into Tb-*meso*-MOF enhancing its catalytic activity, presumably because it preserves its hydrophobic interactions towards MOFs. It was
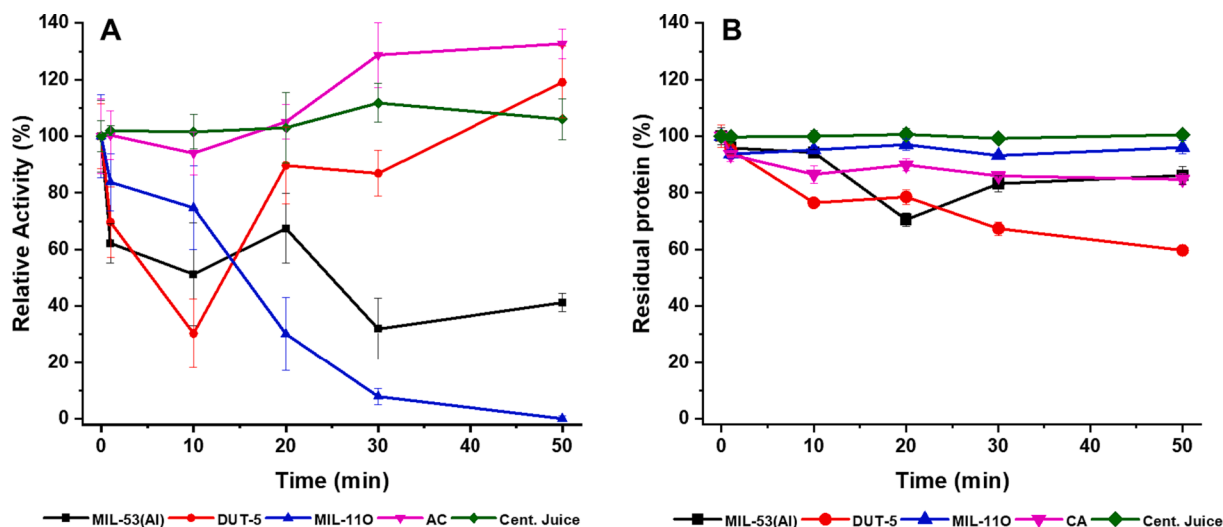

Fig. 2. Effect of Al-based-MOFs and AC on A) PPO relative activity and B) residual protein content of apple juice at t = 0–50 min (values are means of three replicates).

found that there are strong π-π interactions between MOF ligand and the hemo group in microperoxidase, banning protein lixiviation. In 2012 Cytochrome *C* was loaded into the same material, experiencing conformational changes to fit Tb-*meso*-MOF cavities (Mehta, Bhardwaj, Bhardwaj, Kim, & Deep, 2016).

According to this, Al-based-MOFs-PPO interactions could be of surface adsorption type, observing fluctuations in kinetics experiments due to adsorption/lixiviation effects (Fig. 2**B**) (Gkaniatsou et al., 2017). MIL-53(Al) exhibited this effect presenting a maximum protein adsorption at t = 20 min, diminishing adsorbed protein at longer times. In Fig. 2**A** it could be appreciated that PPO activity in juice keeps low, evidencing that MIL-53(Al) interacts with PPO in such a way that no matter that the protein is again released in the media, does not recover its activity. DUT-5 and AC materials retain more protein (≈40%), with low inactivation effects. Therefore, the selectivity for these two materials to inactivate PPO is low and perhaps the adsorbed proteins are from a different kind or the PPO-MOF interaction does not modify enzyme activity.

In comparison, MIL-110 does not exhibit the latter effects but inactivates PPO, which is the desirable result, also retains fewer protein contents, and the adsorption/lixiviation fluctuations are smaller. These results are favorable because these MOF-PPO interactions are enough to inactivate PPO, avoid enzymatic browning, diminish the retention of proteins, and keep juice nutrients.

3.1.2. Juice characterization

Physicochemical characterization data of apple juice after interaction with the materials (X-J) are shown in Table 1. There was no significant difference in density, pH and soluble solids, before and after interaction, e.g. soluble solids content remained constant, and the dissolved sugars did not interact significantly with the adsorbent materials. Regarding density, a slight decrease was observed after the interaction with the materials being the highest deviation about 1.3% for AC-J, and 0.7% for Al-based-MOFs (DUT-5-J), this agrees with the MOF that adsorbed more protein (Fig. 2**B**). Concerning the pH, a slight increase (around 1%) can be observed after the adsorption process. All the values obtained from the measured parameters agree with Mexican regulation (NMX-045–1982 ("NMX-F-045-1982. Alimentos frutas y derivados, Jugo de manzana. Foods, Fruits and derivatives, apple juice normas mexicanas.," 1982)) for commercial apple juices, which is highly desirable in a production scheme with a new technology (Su & Wiley, 1998).

PPO inhibition with Al-based-MOFs has advantages at two levels, according to i) physical treatments, and ii) common inhibitors/additives, as will be discussed. Al-based-MOFs treatments are carried out at room temperature, expending less energy, avoiding the loss of thermolabile nutrients, especially vitamin C; changes in color and flavor generated by both normal heating and microwave processes (Marrufo-Hernández et al., 2017; Su & Wiley, 1998), also having good physicochemical characteristics after adsorption. The materials are completely removed from the juice by filtration after the interaction times, guaranteeing the safety of the juice being MOF-free. This since ascorbic acid is the only antioxidant (juice additive) allowed by Mexican regulation (NMX-F-045-1982 ("NMX-F-045-1982. Alimentos frutas y derivados,

Table 1

Physicochemical characteristics of apple juice before and after the adsorption process.

Parameter/Sample	Density (g/mL)*	pH*	Soluble solids (°Bx)
Initial Juice	1.067	3.22	13
Centrifuged Juice	1.062	3.16	13
MIL-53(Al)-J	1.061	3.24	13
DUT-5-J	1.060	3.26	13
MIL-110-J	1.061	3.24	13
AC-J	1.053	3.23	13

* Triplicates made all measurements with standard deviation ≤ 5 %. In materials labels "J" indicates Juice after the adsorption procedure.

Jugo de manzana. Foods, Fruits and derivatives, apple juice normas mexicanas.," 1982)) in maximum concentrations of 150 mg·kg^{-1}.

Comparing the inactivation methods used in this work with conventional treatments previously reported, MIL-110 performance is comparable with already tested inhibitors, such as sodium metabisulfite (1 mM), ascorbic acid (1 mM), and tropolone (10 mM), also with thermal (80 °C in 5 min) and microwave (140 W in 60 s), which successfully inactivated PPO. Likewise, PPO inactivation with MIL-53(Al) and DUT-5, occurred up to 30% in short times (t < 30 min), comparable with kojic acid (10 mM), and better than the rest (EDTA, succinic acid, benzoic acid, potassium sorbate, and NaCl), ranging 40–70% at the maximum concentrations analyzed (10 mM) (Marrufo-Hernández et al., 2017).

3.2. Analysis of the adsorbent materials before and after the interaction with catechol-type substrates and apple juice
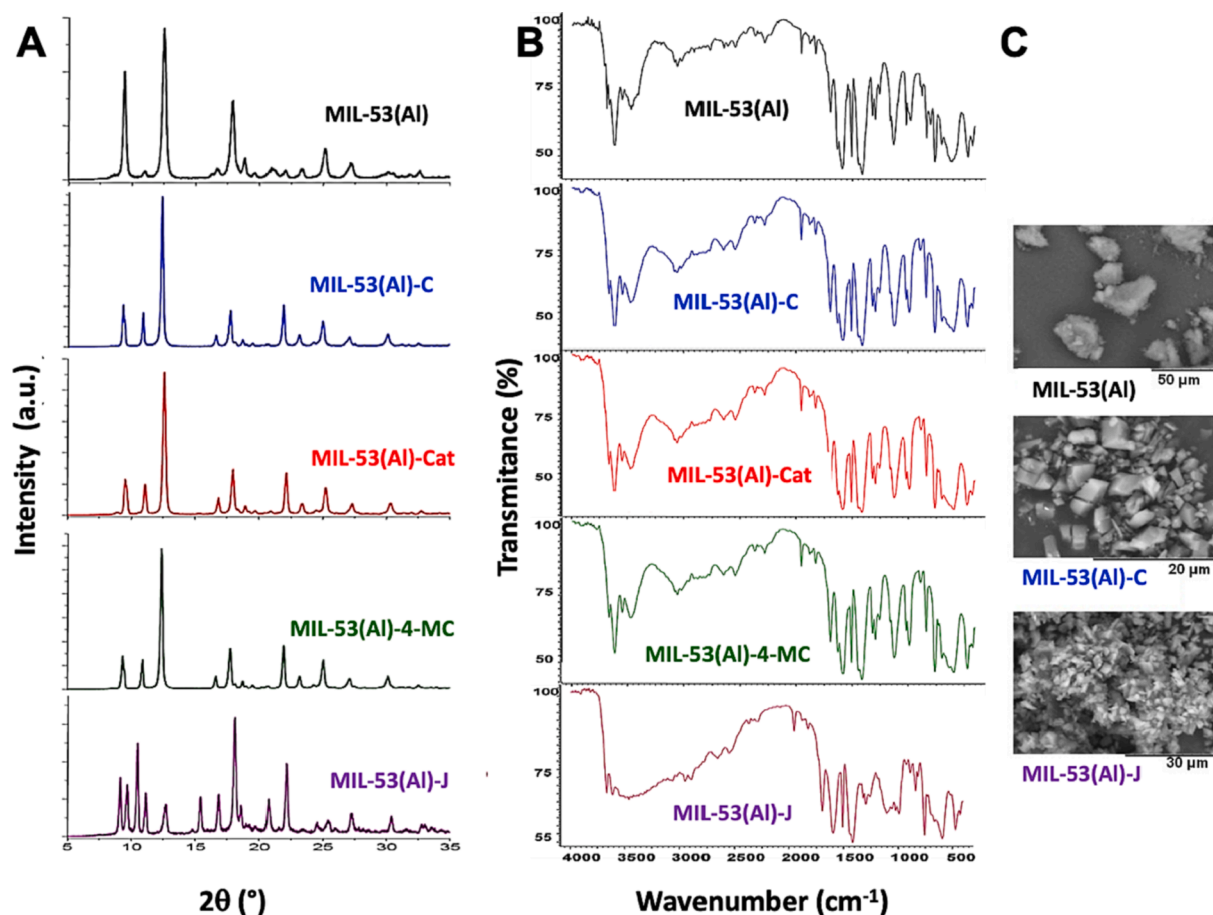
3.2.1. MOF MIL-53(Al)

XRD of MIL-53(Al) (Fig. 3**A**, black), has the corresponding peaks (9.3-30°) of the phases "*lt*" (low-temperature) and "*as*" (as-synthesized) (Loiseau et al., 2004). FTIR (Fig. 3**B**, black) shows the bands at 1590 and 1506, 1443 and 1411 cm^{-1} of COO-Al asymmetric/symmetric stretching. The bands at 3700–3000 and 1632 cm^{-1} are OH of occluded water, and the band at 1679 cm^{-1} corresponds to C=O of uncoordinated terephthalic acid, confirming the "*as*" phase (Loiseau et al., 2004; Patil et al., 2011; Rallapalli et al., 2010). SEM shows crystals of different sizes, all <30 μm with not well-defined morphologies but with good crystallinity according to XRD.

XRD of MIL-53(Al)-C (Fig. 3**A**, blue) shows an increased amount of water since the peaks at 12.5 and 25.2° exclusive for the "*lt*" phase, have higher intensity, and to a lesser extent some peaks (9.4, 10.9, 17.9 and 22.0°) belong to the "*as*" phase. FTIR (Fig. 3**B**, blue) shows a slight increase in the bands at 3612, 3542, 1632, and 1122 cm^{-1} corresponding to OH of occluded water molecules and Al-SBUs of MOF (Loiseau et al., 2004). SEM (Fig. 3**C**) evidenced a crystal size reduction of MIL-53(Al)-C (≈8 and ≈2 μm), compared with MIL-53(Al), preserving the morphology.

XRD of MIL-53(Al)-Cat (red), and MIL-53(Al)-4-MC (green) (Fig. 3**A**), shows that crystalline phases remain in similar proportions, decreasing the intensities of the peaks at 9.4, 10.9, 12.5, 17.9, 22.0 and 25.2°. An order of intensity has been observed: MIL-53(Al)-C > MIL-53(Al)-4-MC > MIL-53(Al)-Cat, and the peaks at 16.7, and 27.3° remained with similar intensity. Changes in 12.5 and 25.2° ("*lt*") peaks correspond to water molecules displacement caused by Cat or 4-MC (Fig. 3**A**) (Loiseau et al., 2004), the least intense being Cat, which was lower adsorbed compared with 4-MC (Fig. 1). The peak at 17.9° ("*as*") increased, corresponding to Cat or 4-MC plus water contents, this effect was also observed in loading ferrocene in MIL-53(Al) (Meilikhov, Yusenko, & Fischer, 2009). FTIR (Fig. 3**B**, red, and green) depicts an increase in the intensity in bands between 1700 and 400 cm^{-1} due to the presence of the substrates, being higher for MIL-53(Al)-4-MC, agreeing with XRD and adsorption observations. Carbonyl bands for *p*-benzoquinone and methyl-*p*-benzoquinone are between 1600 and 1590 cm^{-1}, overlapping with COO-Al bands in MOFs, slightly increasing their intensity ("SDBSWeb: Spectral Database for Organic Compounds SDBS (Access Date: September, 2017),").

XRD of MIL-53(Al)-J (Fig. 3**A**, purple) shows a general decrease in peaks intensity in comparison with MIL-53(Al)-C, nevertheless, all peaks of starting MIL-53(Al) remained, the largest decrease at 12.5 and the smallest at 17.9° peaks indicate a higher quantity of expanded pores due to the occlusion of juice molecules into MOF. FTIR (Fig. 3**B**, purple), revealed a general broadening in the OH area (3700–3000 cm^{-1}), the 3685 and 3665 cm^{-1} bands are preserved, as well as material coordination bands (1590–1400 cm^{-1}), confirming XRD observations. Bands at 1632 and 1122 cm^{-1} decreased attributed to occluded water molecules diminishment (Meilikhov et al., 2009). Comparatively, the bands at 1200–1000 cm^{-1} became more intense and wider due to juice

Fig. 3. Characterization by A) XRD, B) FTIR, and C) SEM of MIL-53(Al) as synthesized (black), conditioned (blue), and after adsorption process with Catechol (red), 4-MC (green), and Juice (purple). (For interpretation of the references to color in this figure legend, the reader is referred to the web version of this article.)

saccharides occlusion. SEM (Fig. 3C) evidenced that MIL-53(Al)-J crystals are smaller than those of MIL-53(Al) and MIL-53(Al)-C, besides juice components developed crystal agglomeration, both could be related to the decrease in peak intensities observed by XRD.

3.2.2. MOF DUT-5

XRD of DUT-5 (Fig. 4A, black) shows the main peaks reported for this MOF (2θ of 5-35°, tetragonal *Imma* space group), that unlike MIL-53(Al), these pores are rigid squares (Gotthardt et al., 2015; Senkovska et al., 2009). FTIR (Fig. 4B, black) illustrates the characteristic bands at 1607 and 1435 cm^{-1}, of symmetric/asymmetric stretching of the COO-Al. The band at 1689 cm^{-1} could be attributed to C=O of non-coordinated ligand, indicating more uncoordinated C=O functional groups of the ligand due to the crystal size reduction (Gotthardt et al., 2015; Senkovska et al., 2009).

For DUT-5-C, both the diffractogram and the micrographs (Fig. 4 **captions A and C**) indicate a considerable decrease in the crystallinity of the material. The diffractogram shows a decrease in the characteristic peaks (12.1, 18.1, and 14.2°) and the microstructure changed from rectangular prisms ($\approx$30 μm) to smaller granules ($\approx$1 μm) (Senkovska et al., 2009). FTIR of DUT-5-C revealed slight differences with the initial material (Fig. 4B, black and blue), mainly the increase in intensity at 1689 cm^{-1} was due to crystal size diminishment, exposing free carboxylate groups during the conditioning process. While the bands of the COO-Al (1700–1400 cm^{-1}) remain similar (Fig. 4B blue), maintaining the structure of the material.

XRD of DUT-5-Cat and DUT-5-4MC (Fig. 4A, red and green) revealed an increase in the intensities of peaks at 12.1, 14.2 and 18.1° compared with DUT-5-C (blue). For these materials, a recovery of their crystallinity

was observed, accompanied by the appearance of the peak at 24.2°, all this due to the presence of Cat or 4-MC occluded into the material somehow aiding a crystallinity enhancement (Senkovska et al., 2009). FTIR of DUT-5-Cat and DUT-5–4-MC remained the same as DUT-5-C. The occluded polyphenols were oxidized at the time of characterization, overlapping the quinone carbonyl bands with the MOF carbonyls ("SDBSWeb: Spectral Database for Organic Compounds SDBS (Access Date: September, 2017)").

The characterization of DUT-5-J is shown in Fig. 4 (purple). XRD exhibited significant changes, peaks at 12.1 and 14.2° disappeared, while an intense peak appeared at 16.7° and the peaks at 24.2, 25.0 and 25.7° became sharper. It is known that the peak at $\approx$24° indicates the occlusion of molecules in the MOF, these new peaks could coincide with the variety of juice components. FTIR shows an increase in the relative intensity of the band at 1688 cm^{-1} which is now more intense than the coordination bands of the binder with aluminum. Likewise, the appearance of a small shoulder is observed at 1589 cm^{-1} and the appearance of the broadband at 1055 cm^{-1} comes from the sugars and components of apple juice (Gabriel, Prestes, Pinheiro, Barison, & Wosiacki, 2013). SEM (Fig. 4C) of DUT-5-C and DUT-5-J revealed that the size and morphology of the crystals are preserved, although by XRD another phase was determined. Contrasting with that observed for MIL-53(Al)-J, maintaining the main peaks, but decreasing their size.

3.2.3. MOF MIL-110

XRD of MIL-110 (Fig. 5A, black), evidences the crystalline structure and space group *P*-62c, with peaks corresponding to the crystalline phase at 8.3 and 17.1° (Haouas et al., 2012). FTIR (Fig. 5B, black) the coordination bands of COO-Al are observed at 1625 and 1589, 1465, and
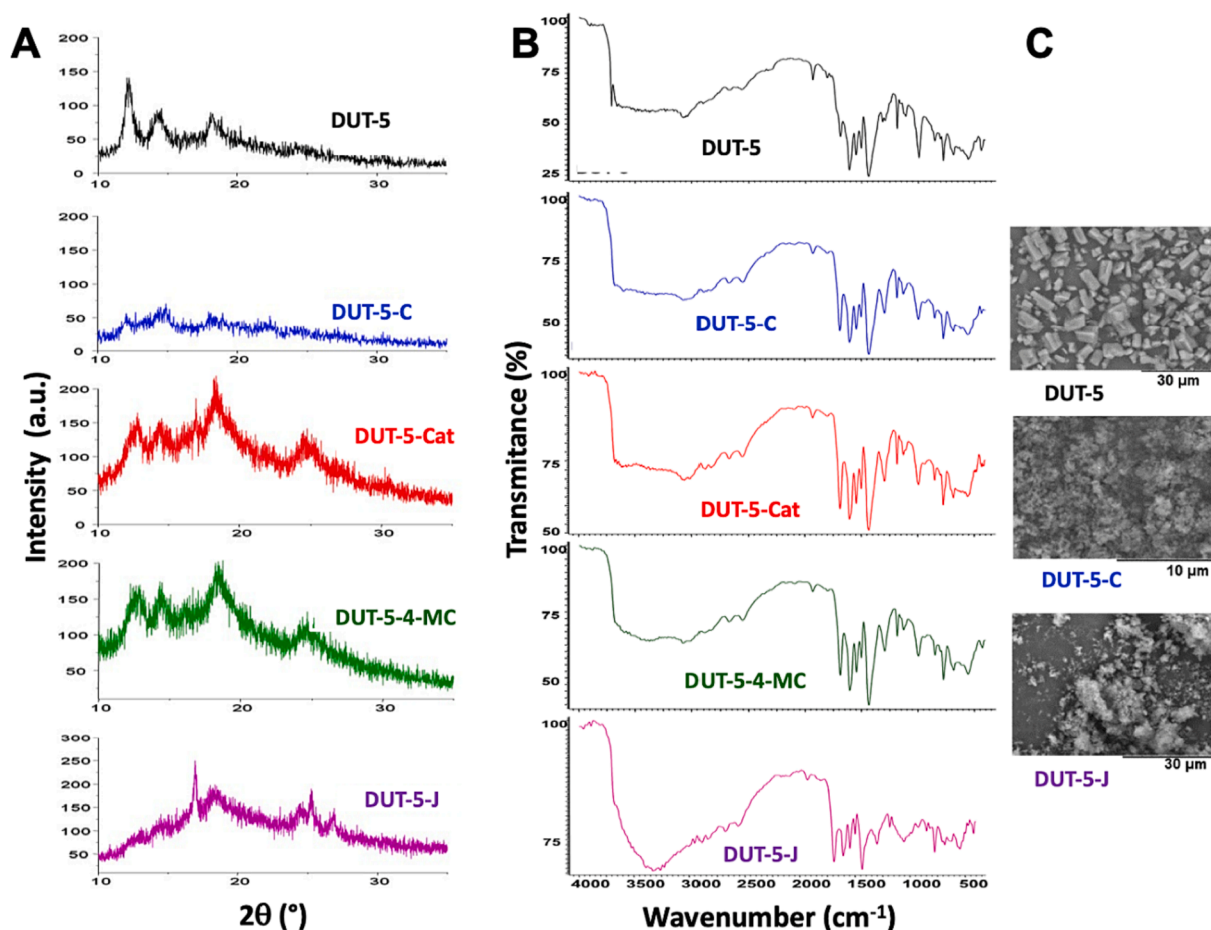
Fig. 4. Characterization by A) XRD, B) FTIR, and C) SEM of DUT-5 as synthesized (black), conditioned (blue), and after adsorption process with Catechol (red), 4-MC (green), and Juice (purple). (For interpretation of the references to color in this figure legend, the reader is referred to the web version of this article.)

1409 cm^{-1} (asymmetric/symmetric stretching). The OH band appears at 3600 to 2600 cm^{-1} corresponding to atmospheric water and uncoordinated carboxylates, with a small shoulder at 1674 cm^{-1} of C=O from trimesic acid (Gerbaldi et al., 2014). SEM (Fig. 5C) confirms the formation of MIL-110 phase by the presence of crystals in the form of hexagonal prisms (Haouas et al., 2012).

XRD of MIL-110-C (Fig. 5A, blue) evidenced retaining its crystalline form and spectroscopic properties (Haouas et al., 2012) and decreased the intensity compared with MIL-110. In FTIR Fig. 5B, an increase in the OH band (3600–3200 cm^{-1}) is observed due to a higher amount of water in the material. SEM (Fig. 5C) verified that the structure and shape of the crystals were maintained after conditioning.

XRD of MIL-110-Cat (red) and MIL-110–4-MC (green) are shown in Fig. 5, noting that these samples were the least structurally affected in comparison with other MOFs. XRD of MIL-110-Cat (Fig. 5A, red), evidenced that the peaks were maintained in their position by modulating the intensities, the peak at 8.3° decreased ≈30 %, while peaks at 17.1 and 19.7° increased ≈10 and 70%, due to the presence of catechol molecules inside the pores (Haouas et al., 2012). A decrease in the FTIR (Fig. 5B, red) OH bands (3600–2600 cm^{-1}) is observed due to the displacement of water molecules by catechol molecules. As previously, catechol oxidation to quinone is observed as a slight increase in the shoulder at 1674 cm^{-1} (carbonyls) (Gerbaldi et al., 2014), and similar compounds appear between 1650 and 1678 cm^{-1} ("SDBSWeb: Spectral Database for Organic Compounds SDBS (Access Date: September, 2017),").

XRD of MIL-110–4-MC (Fig. 5A, green) shows the main peak shifted from 8.3 to 8.7° and decreased intensity ≈47%, the peak at 9.5° disappeared, and the peak at 12.6 shifted to 13°, recovering ≈80% intensity

with respect to MIL-110-C. In FTIR (Fig. 5B, green) the band at 1674 cm^{-1} increased, as well as the shoulder at 1558 cm^{-1}, due to C=O of the adsorbed methyl-*o*-benzoquinone ("SDBSWeb: Spectral Database for Organic Compounds SDBS (Access Date: September, 2017),"), and a decrease in the OH band was observed. The MIL-110 adsorbed a similar amount of the two substrates (Fig. 1), indicating that the inactivation of the PPO should not be related to the adsorption of the substrates, but to the protein-MOF interaction.

In XRD of MIL-110-J (Fig. 5A, purple) could be seen that, unlike DUT-5-J, this material presents the same peaks before and after adsorption, and like MIL-53-J there is a diminishment of peaks intensities and crystal size attributed to a different selectivity of the MOF for compounds of the juice. Similarly, for MIL-110–4-MC, the peak at 9.4° disappeared and the one at 8.3° shifted to 8.7°, there were observed diminishments in peak intensities of ≈50%, except for the peak by 12.1°, increasing its intensity with respect to the MIL-110-C. FTIR (Fig. 5B purple) evidenced OH band increasing with respect to MIL-110-C (blue). Unlike, MIL-110-Cat and MIL-110–4-MC, for MIL-110-J the band at 1674 cm^{-1} (C=O quinones) was not modified. Agreeing with MIL-53 (Al)-J and DUT-5-J, a broad band appeared at 1055 cm^{-1}, due to sugars in apple juice (Gabriel, Prestes, Pinheiro, Barison, & Wosiacki, 2013). SEM (Fig. 5C) exhibited MIL-110-J crystals retaining shape and size, likewise, crystal agglomeration of MOF-juice components was observed. This material is the least affected through physicochemical and morphological characteristics for all tested MOFs.

Finally, and based on current results, it could be summarized that MIL-110 inactivated PPO in 50 min, while DUT-5 and MIL-53(Al) reduced PPO activity by up to 70%, DUT-5 adsorbed the most protein, and the best substrates adsorbents were MIL-110 and DUT-5. All
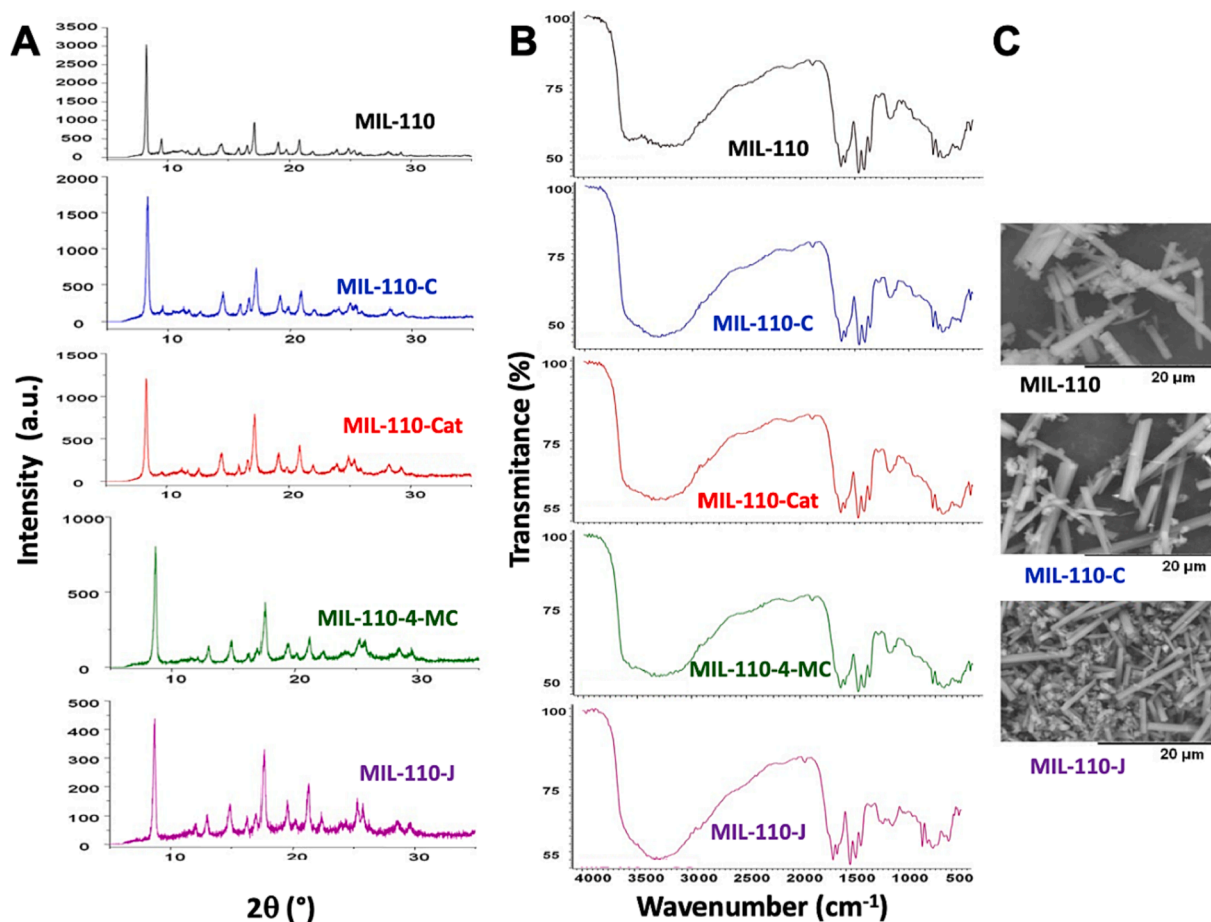
Fig. 5. Characterization by A) XRD, B) FTIR, and C) SEM of MIL-110 as synthesized (black), conditioned (blue), and after adsorption process with Catechol (red), 4-MC (green), and Juice (purple). (For interpretation of the references to color in this figure legend, the reader is referred to the web version of this article.)

materials preserved their crystalline structure, but the intensities decreased except for some peaks. The spectroscopic properties were also maintained after conditioning and adsorption processes, both for substrates and for juice. Noteworthy, MIL-110 provided the best characteristics, adsorbing the least amount of protein and completely inactivating PPO, also preserving the nutritional values of the juice, as a very desirable characteristic of the final product. All this answers the initial statement/hypothesis that the water-stable Al-based-MOFs could be good promising/innovative materials for industrial apple juice processing at room temperature, and enzyme inactivation processes, e.g., PPO, that potentially be extended to other food matrices.

3.3. Perspectives for anti-browning applicability of Al-based MOFs

Since the current research was originally aimed at the possible employment of Al-based MOFs to achieve an anti-browning effect in apple juice, qualitative pieces of evidences of the obtained results were included in Fig. 6. In this visual material resulted easy to notice that by the time lapse of the experiment in captions A) t = 1 min (filtered), B) t = 1 min (unfiltered), C) t = 30 min (filtered), C) t = 30 min (unfiltered), and E) t = 4 months (filtered), the browning inhibition effect was achieved for all the tested Al-based-MOFs, being the MIL-110 material, the one with better effect. In panel D) for the centrifuged juice it could be noticed the natural browning effect when the juice is untreated. A very important evidence is placed in caption E) where samples were stored for 4 months at 4 °C, to slow down or minimize enzymatic activity and to assess the shelf-life of the studied systems. The centrifuged juice sample, accompanied by AC treated sample ended with a more pronounced browning effect in comparison with the Al-based-MOF treated samples,

therefore evidencing the inhibition/inactivation of PPO as was initially stated for this study.

Once the most important characteristics were fulfilled, the possibility for an industrial application is now dependent on production costs, scaling, and process optimization among other variables for the use of MOF in the juice processing (Eddaoudi et al., 2015; Kong & Li, 2021). Therefore the following aspects should be considered: 1) within the juice production process, filtration and centrifugation operations are included (Girard, Fukumoto, & Sefa Koseoglu, 2000), so the use of MOF could be easily adapted to the existing process; 2) Many MOFs are becoming commercial materials and even commodities, therefore their costs are variable, e.g. one of the most easily accessible is MIL-53(Al) that would be purchased at prices from *ca.* 18.00 USD per gram (https://www.si gmaaldrich.com/MX/es/product/aldrich/688738) or even be synthesized at lower prices if needed; 3) MOF after adsorption would be washed with non-concentrated solvents or acids to be reused and thus also reduce costs (Huo & Yan, 2012; Patil et al., 2011), e.g. it has been reported that MOF MIL-53 (Al) could be reused from three (Patil et al., 2011) to twelve times (Liu et al., 2016) with yields of 90% after the conditioning process; 4) if MOF adsorption process could be scalable, around 0.5 g of MOF would be enough to inactivate PPO present in 1 L of juice; and 5) to make MOFs more attractive, optimization studies with different MOF-Juice ratios could be developed to try to reduce operating times and costs.

4. Conclusions

The materials that adsorbed the most substrates and protein were MOF DUT-5, followed by MIL-53(Al), but they were not able to
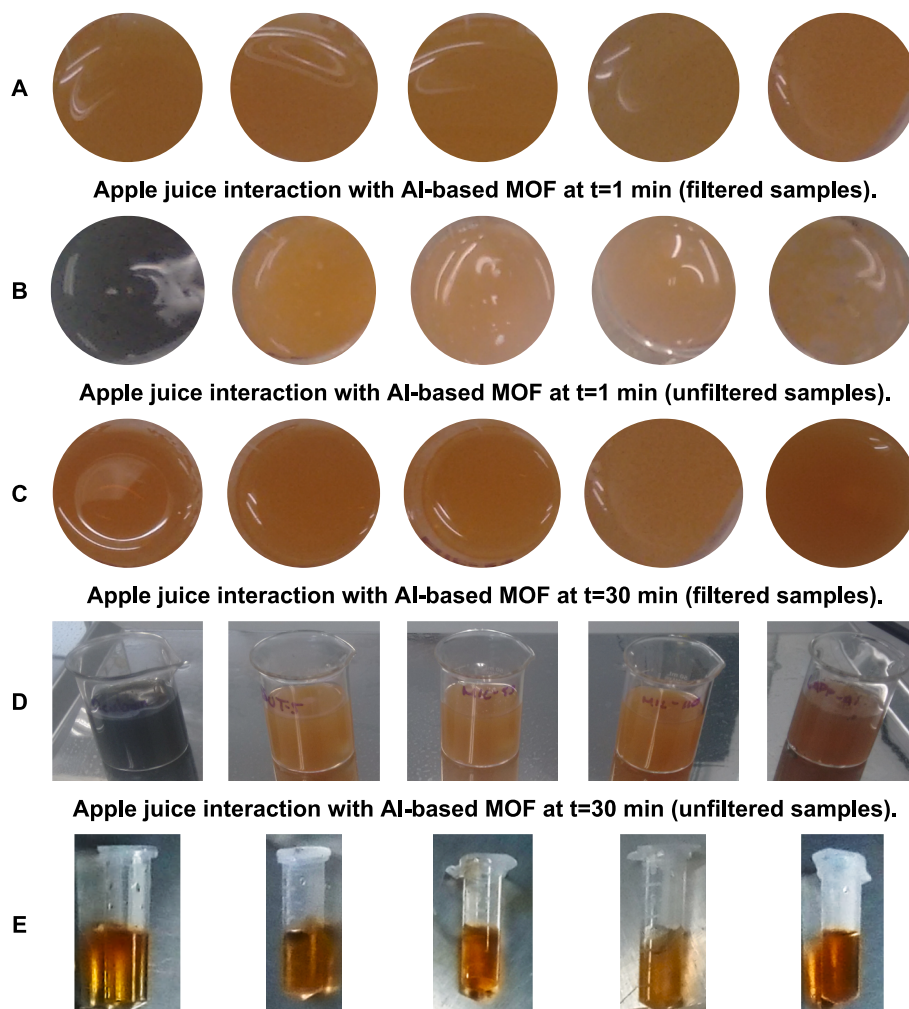
Fig. 6. Apple juice aspect by interaction with Al-based MOF at: A) t = 1 min (filtered samples); B) t = 1 min (unfiltered samples); C) t = 30 min (filtered samples); D) t = 30 min (unfiltered samples); E) t = 4 months of storage at 4 °C (filtered samples); against centrifuged juice as reference.

inactivate PPO, reducing the relative activity up to 70% in short interaction times (<30 min), so the inactivation of the enzyme is not carried out under these conditions. Notably, the MOF MIL-110 is a moderate adsorbent of substrates and the lowest protein adsorbent, but it was the only one capable of inactivating PPO. This indicates that the inactivation of the enzyme should be carried out through MOF-PPO interactions. From the characterization of the juice after the adsorption process, it was shown that it preserves the desired physicochemical and nutritional properties, while the materials maintain their structural properties. MIL-110 turned out to be a good enzyme inactivator, such as PPO, and a good apple juice clarifier agent, and its use would be extended to other food matrices as well. Therefore further work is needed precisely to evaluate the stability and reusability of these MOFs under different conditions and to explore their potential applications in other types of juices and beverages.

CRediT authorship contribution statement

Norma A. Marrufo-Hernández: Conceptualization, Data curation, Formal analysis, Investigation, Methodology, Software, Validation, Writing – original draft, Writing – review & editing. **Hugo Nájera:** Conceptualization, Formal analysis, Funding acquisition, Investigation, Methodology, Project administration, Resources, Supervision, Validation, Writing – original draft, Writing – review & editing. **Fernando González-Chávez:** Conceptualization, Data curation, Formal analysis, Investigation, Methodology, Writing – original draft. **Hiram I. Beltrán:** Conceptualization, Formal analysis, Funding acquisition, Investigation, Methodology, Project administration, Resources, Supervision, Validation, Writing – original draft, Writing – review & editing.

Declaration of competing interest

The authors declare that they have no known competing financial interests or personal relationships that could have appeared to influence the work reported in this paper.

Data availability

Data will be made available on request.

Acknowledgement

References

Aguliar Perez, K. M., Alagoz, Y., Maatouk, B., Wang, J. Y., Berqdar, L., Qutub, S., … Khashab, N. M. (2023). Biomimetic mineralization for smart biostimulant delivery

and crop micronutrients fortification. *Nano Letters, 23*(11), 4732–4740. https://doi.org/10.1021/acs.nanolett.2c04506

Bai, J.-W., Gao, Z.-J., Xiao, H.-W., Wang, X.-T., & Zhang, Q. (2013). Polyphenol oxidase inactivation and vitamin C degradation kinetics of Fuji apple quarters by high humidity air impingement blanching. *International Journal of Food Science & Technology, 48*(6), 1135–1141. https://doi.org/10.1111/j.1365-2621.2012.03193.x

Barreto, A. S., da Silva, R. L., dos Santos Silva, S. C. G., Rodrigues, M. O., de Simone, C. A., de Sá, G. F., … de Mesquita, M. E. (2010). Potential of a metal–organic framework as a new material for solid-phase extraction of pesticides from lettuce (Lactuca sativa), with analysis by gas chromatography-mass spectrometry. *Journal of Separation Science, 33*(23–24), 3811–3816. https://doi.org/10.1002/jssc.201000553

Bollag, D. M., Rozycki, M. D., & Edelstein, S. J. (1996). *Protein methods* ((2nd ed.)). New York: Wiley-Liss.

Chauhan, D., Omar, R. A., Mangalaraja, R. V., Ashfaq, M., & Talreja, N. (2022). Chapter 13 - Metal-organic framework as an emerging material: A novel plant growth stimulant. In G. M. Balestra, & E. Fortunati (Eds.), *Nanotechnology-Based Sustainable Alternatives for the Management of Plant Diseases* (pp. 323–339). Elsevier.

Chen, X.-F., Zang, H., Wang, X., Cheng, J.-G., Zhao, R.-S., Cheng, C.-G., & Lu, X.-Q. (2012). Metal-organic framework MIL-53(Al) as a solid-phase microextraction adsorbent for the determination of 16 polycyclic aromatic hydrocarbons in water samples by gas chromatography-tandem mass spectrometry. *The Analyst, 137*(22), 5411–5419. https://doi.org/10.1039/C2AN35806A

Devece, C., Rodriguez-Lopez Jn Fau - Fenoll, L. G., Fenoll Lg Fau - Tudela, J., Tudela J Fau - Catala, J. M., Catala Jm Fau - de Los Reyes, E., de Los Reyes E Fau - Garcia-Canovas, F., & Garcia-Canovas, F. (1999). Enzyme inactivation analysis for industrial blanching applications: Comparison of microwave, conventional, and combination heat treatments on mushroom polyphenoloxidase activity. (0021-8561 (Print)).

Eddaoudi, M., Sava, D. F., Eubank, J. F., Adil, K., & Guillerm, V. (2015). Zeolite-like metal-organic frameworks (ZMOFs): Design, synthesis, and properties. *Chemical Society Reviews, 44*(1), 228–249. https://doi.org/10.1039/C4CS00230J

Ettlinger, R., Lachelt, U., Gref, R., Horcajada, P., Lammers, T., Serre, C., … Wuttke, S. (2022). Toxicity of metal-organic framework nanoparticles: From essential analyses to potential applications. *Chemical Society Reviews, 51*(2), 464–484. https://doi.org/10.1039/d1cs00918d

Fan, W., Wang, K.-Y., Welton, C., Feng, L., Wang, X., Liu, X., … Sun, D. (2023). Aluminum metal–organic frameworks: From structures to applications. *Coordination Chemistry Reviews, 489*. https://doi.org/10.1016/j.ccr.2023.215175

Fu, Y., Yang, D., Chen, Y., Shi, J., Zhang, X., Hao, Y., … Zhang, J. (2023). MOF-based active packaging materials for extending post-harvest shelf-life of fruits and vegetables. *Materials (Basel), 16*(9). https://doi.org/10.3390/ma16093406

Fu, Y., Zhang, K., Wang, N., & Du, J. (2007). Effects of aqueous chlorine dioxide treatment on polyphenol oxidases from Golden Delicious apple. *LWT - Food Science and Technology, 40*(8), 1362–1368. https://doi.org/10.1016/j.lwt.2006.11.001

Gabriel, L. S., Prestes, R. A., Pinheiro, L. A., Barison, A., & Wosiacki, G. (2013). Multivariate analysis of the spectroscopic profile of the sugar fraction of apple pomace. *Brazilian Archives of Biology and Technology, 56*, 439–446. https://doi.org/10.1590/S1516-89132013000300012

Genovese, D. B., Elustondo, M. P., & Lozano, J. E. (1997). Color and cloud stabilization in cloudy apple juice by steam heating during crushing. *Journal of Food Science, 62*(6), 1171–1175. https://doi.org/10.1111/j.1365-2621.1997.tb12238.x

Gerbaldi, C., Nair, J. R., Kulandainathan, M. A., Kumar, R. S., Ferrara, C., Mustarelli, P., & Stephan, A. M. (2014). Innovative high performing metal organic framework (MOF)-laden nanocomposite polymer electrolytes for all-solid-state lithium batteries. *Journal of Materials Chemistry A, 2*(26), 9948–9954. https://doi.org/10.1039/C4TA01856G

Girard, B., Fukumoto, L. R., & Sefa Koseoglu, S. (2000). Membrane processing of fruit juices and beverages: A review. *Critical Reviews in Biotechnology, 20*(2), 109–175. https://doi.org/10.1080/07388550008984168

Gkaniatsou, E., Sicard, C., Ricoux, R., Mahy, J.-P., Steunou, N., & Serre, C. (2017). Metal-organic frameworks: A novel host platform for enzymatic catalysis and detection. *Materials Horizons, 4*(1), 55–63. https://doi.org/10.1039/C6MH00312E

Gotthardt, M. A., Grosjean, S., Brunner, T. S., Kotzel, J., Ganzler, A. M., Wolf, S., … Kleist, W. (2015). Synthesis and post-synthetic modification of amine-, alkyne-, azide- and nitro-functionalized metal-organic frameworks based on DUT-5. *Dalton Transactions, 44*(38), 16802–16809. https://doi.org/10.1039/C5DT02276B

Grall, R., Hidalgo, T., Delic, J., Garcia-Marquez, A., Chevillard, S., & Horcajada, P. (2015). In vitro biocompatibility of mesoporous metal (III; Fe, Al, Cr) trimesate MOF nanocarriers. *Journal of Materials Chemistry B, 3*(42), 8279–8292. https://doi.org/10.1039/c5tb01223f

Haouas, M., Volkringer, C., Loiseau, T., Férey, G., & Taulelle, F. (2012). In situ NMR, ex situ XRD and SEM study of the hydrothermal crystallization of nanoporous aluminum trimesates MIL-96, MIL-100, and MIL-110. *Chemistry of Materials, 24*(13), 2462–2471. https://doi.org/10.1021/cm300439e

Haque, E., Lo, V., Minett, A. I., Harris, A. T., & Church, T. L. (2014). Dichotomous adsorption behaviour of dyes on an amino-functionalised metal-organic framework, amino-MIL-101(Al). *Journal of Materials Chemistry A, 2*(1), 193–203. https://doi.org/10.1039/C3TA13589F

Hasan, Z., Khan, N. A., & Jhung, S. H. (2016). Adsorptive removal of diclofenac sodium from water with Zr-based metal–organic frameworks. *Chemical Engineering Journal, 284*, 1406–1413. https://doi.org/10.1016/j.cej.2015.08.087

Huo, S.-H., & Yan, X.-P. (2012). Metal-organic framework MIL-100(Fe) for the adsorption of malachite green from aqueous solution. *Journal of Materials Chemistry, 22*(15), 7449–7455. https://doi.org/10.1039/C2JM16513A

Illera, A. E., Chaple, S., Sanz, M. T., Ng, S., Lu, P., Jones, J., … Bourke, P. (2019). Effect of cold plasma on polyphenol oxidase inactivation in cloudy apple juice and on the

quality parameters of the juice during storage. *Food Chemistry: X, 3*, Article 100049. https://doi.org/10.1016/j.fochx.2019.100049

Iqbal, A., Murtaza, A., Hu, W., Ahmad, I., Ahmed, A., & Xu, X. (2019). Activation and inactivation mechanisms of polyphenol oxidase during thermal and non-thermal methods of food processing. *Food and Bioproducts Processing, 117*, 170–182. https://doi.org/10.1016/j.fbp.2019.07.006

Islamoglu, T., Chen, Z., Wasson, M. C., Buru, C. T., Kirlikovali, K. O., Afrin, U., … Farha, O. K. (2020). Metal-organic frameworks against toxic chemicals. *Chemical Reviews, 120*(16), 8130–8160. https://doi.org/10.1021/acs.chemrev.9b00828

Janovitz-Klapp, A., Richard, F., & Nicolas, J. (1989). Polyphenoloxidase from apple, partial purification and some properties. *Phytochemistry, 28*(11), 2903–2907. https://doi.org/10.1016/0031-9422(89)80250-X

Kong, X.-J., & Li, J.-R. (2021). An overview of metal-organic frameworks for green chemical engineering. *Engineering, 7*(8), 1115–1139. https://doi.org/10.1016/j.eng.2021.07.001

Li, L., Yuan, L. J., Hong, W., Fan, L., Mao, L. B., & Liu, L. (2015). Hybrid Fe_3O_4/MOFs for the adsorption of methylene blue and methyl violet from aqueous solution. *Desalination and Water Treatment, 55*(7), 1973–1980. https://doi.org/10.1080/19443994.2014.937751

Liang, J., Zulkifli, M. Y. B., Choy, S., Li, Y., Gao, M., Kong, B., … Liang, K. (2020). Metal-organic framework-plant nanobiohybrids as living sensors for on-site environmental pollutant detection. *Environmental Science & Technology, 54*(18), 11356–11364. https://doi.org/10.1021/acs.est.0c04688

Liu, F., Zhao, J.-H., Gan, Z.-L., & Ni, Y.-Y. (2015). Comparison of membrane-bound and soluble polyphenol oxidase in Fuji apple (Malus domestica Borkh. cv. Red Fuji). *Food Chemistry, 173*, 86–91. https://doi.org/10.1016/j.foodchem.2014.09.169

Liu, X., Feng, T., Wang, C., Hao, L., Wang, G., Wu, Q., & Wang, Z. (2016). A metal-organic framework-derived nanoporous carbon/iron composite for enrichment of endocrine disrupting compounds from fruit juices and milk samples. *Analytical Methods, 8*(17), 3528–3535. https://doi.org/10.1039/C6AY00191B

Loiseau, T., Serre, C., Huguenard, C., Fink, G., Taulelle, F., Henry, M., … Férey, G. (2004). A rationale for the large breathing of the porous aluminum terephthalate (MIL-53) upon hydration. *Chemistry – A European Journal, 10*(6), 1373–1382. https://doi.org/10.1002/chem.200305413

Lopez, P., Sala, F. J., de la Fuente, J. L., Condon, S., Raso, J., & Burgos, J. (1994). Inactivation of peroxidase, lipoxygenase, and polyphenol oxidase by manothermosonication. *Journal of Agricultural and Food Chemistry, 42*(2), 252–256. https://doi.org/10.1021/jf00038a005

Majewski, M. B., Noh, H., Islamoglu, T., & Farha, O. K. (2018). NanoMOFs: Little crystallites for substantial applications. *Journal of Materials Chemistry A, 6*(17), 7338–7350. https://doi.org/10.1039/c8ta02132e

Makroo, H. A., Saxena, J., Rastogi, N. K., & Srivastava, B. (2017). Ohmic heating assisted polyphenol oxidase inactivation of watermelon juice: Effects of the treatment on pH, lycopene, total phenolic content, and color of the juice. *Journal of Food Processing and Preservation*, e13271-n/a. https://doi.org/10.1111/jfpp.13271

Marrufo-Hernández, N. A., Palma-Orozco, G., Beltrán, H. I., & Nájera, H. (2017). Purification, partial biochemical characterization and inactivation of polyphenol oxidase from Mexican Golden Delicious apple (Malus domestica). *Journal of Food Biochemistry*, e12356. https://doi.org/10.1111/jfbc.12356

Mayer, A. M. (2006). Polyphenol oxidases in plants and fungi: Going places? A review. *Phytochemistry, 67*(21), 2318–2331. https://doi.org/10.1016/j.phytochem.2006.08.006

Mehta, J., Bhardwaj, N., Bhardwaj, S. K., Kim, K.-H., & Deep, A. (2016). Recent advances in enzyme immobilization techniques: Metal-organic frameworks as novel substrates. *Coordination Chemistry Reviews, 322*(Supplement C), 30–40. https://doi.org/10.1016/j.ccr.2016.05.007

Meilikhov, M., Yusenko, K., & Fischer, R. A. (2009). The adsorbate structure of ferrocene inside [Al(OH)(bdc)]x (MIL-53): A powder X-ray diffraction study. *Dalton Transactions, 4*, 600–602. https://doi.org/10.1039/B820882B

Ni Eidhin, D. M., Murphy, E., & O'Beirne, D. (2006). Polyphenol Oxidase from Apple (Malus domestica Borkh. cv Bramley's Seedling): Purification strategies and characterization. *Journal of Food Science, 71*(1), C51–C58. https://doi.org/10.1111/j.1365-2621.2006.tb12388.x

NMX-F-045-1982. Alimentos frutas y derivados, Jugo de manzana. Foods, Fruits and derivatives, apple juice normas mexicanas. (1982). (p. 5). http://www.colpos.mx/bancodenormas/nmexicanas/NMX-F-045-1982.PDF. Dirección General de Normas Comerciales.

Norma general del CODEX para zumos (jugos) y néctares de frutas (CODEX STAN 247-2005). (2005).

Núñez-Gastélum, J. A., Alvarez-Parrilla, E., de la Rosa, L. A., Martínez-Ruíz, N. R., González-Aguilar, G. A., & Rodrigo-García, J. (2015). Effect of harvest date and storage duration on chemical composition, sugar and phenolic profile of 'Golden Delicious' apples from northwest Mexico. *New Zealand Journal of Crop and Horticultural Science, 43*(3), 214–221. https://doi.org/10.1080/01140671.2015.1026358

Palma-Orozco, G., Marrufo-Hernandez, N. A., Sampedro, J. G., & Najera, H. (2014). Purification and partial biochemical characterization of polyphenol oxidase from mango (Mangifera indica cv. Manila). *Journal of Agricultural and Food Chemistry, 62*(40), 9832–9840. https://doi.org/10.1021/jf5029784

Palma-Orozco, G., Marrufo-Hernández, N. A., Tobías, I., & Nájera, H. (2019). Purification and biochemical characterization of polyphenol oxidase from soursop (Annona muricata L.) and its inactivation by microwave and ultrasound treatments. *Journal of Food Biochemistry, 43*(3), e12770. https://doi.org/10.1111/jfbc.12770

Palma-Orozco, G., Ortiz-Moreno, A., Dorantes-Alvarez, L., Sampedro, J. G., & Najera, H. (2011). Purification and partial biochemical characterization of polyphenol oxidase

from mamey (*Pouteria sapota*). *Phytochemistry, 72*(1), 82–88. https://doi.org/10.1016/j.phytochem.2010.10.011

Patil, D. V., Rallapalli, P. B. S., Dangi, G. P., Tayade, R. J., Somani, R. S., & Bajaj, H. C. (2011). MIL-53(Al): An efficient adsorbent for the removal of nitrobenzene from aqueous solutions. *Industrial & Engineering Chemistry Research, 50*(18), 10516–10524. https://doi.org/10.1021/ie200429f

Pinar Gumus, Z., & Soylak, M. (2021). Metal organic frameworks as nanomaterials for analysis of toxic metals in food and environmental applications. *TrAC Trends in Analytical Chemistry, 143*. https://doi.org/10.1016/j.trac.2021.116417

Qian, X., Yadian, B., Wu, R., Long, Y., Zhou, K., Zhu, B., & Huang, Y. (2013). Structure stability of metal-organic framework MIL-53 (Al) in aqueous solutions. *International Journal of Hydrogen Energy, 38*(36), 16710–16715. https://doi.org/10.1016/j.ijhydene.2013.07.054

Qin, F.-X., Jia, S.-Y., Liu, Y., Li, H.-Y., & Wu, S.-H. (2015). Adsorptive removal of bisphenol A from aqueous solution using metal-organic frameworks. *Desalination and Water Treatment, 54*(1), 93–102. https://doi.org/10.1080/19443994.2014.883331

Queiroz, C., Mendes Lopes, M. L., Fialho, E., & Valente-Mesquita, V. L. (2008). Polyphenol oxidase: Characteristics and mechanisms of browning control. *Food Reviews International, 24*(4), 361–375. https://doi.org/10.1080/87559120802089332

Rallapalli, P., Patil, D., Prasanth, K. P., Somani, R. S., Jasra, R. V., & Bajaj, H. C. (2010). An alternative activation method for the enhancement of methane storage capacity of nanoporous aluminium terephthalate, MIL-53(Al). *Journal of Porous Materials, 17*(5), 523–528. https://doi.org/10.1007/s10934-009-9320-5

Richardson, J. J., & Liang, K. (2018). Nano-Biohybrids. In vivo synthesis of metal-organic frameworks inside living plants. *Small, 14*(3). https://doi.org/10.1002/smll.201702958

Rojas, S., Rodriguez-Dieguez, A., & Horcajada, P. (2022). Metal-organic frameworks in agriculture. *ACS Applied Materials & Interfaces, 14*(15), 16983–17007. https://doi.org/10.1021/acsami.2c00615

Samokhvalov, A. (2018). Aluminum metal–organic frameworks for sorption in solution: A review. *Coordination Chemistry Reviews, 374*, 236–253. https://doi.org/10.1016/j.ccr.2018.06.011

SDBSWeb: Spectral Database for Organic Compounds SDBS (Access Date: September, 2017). http://sdbs.db.aist.go.jp: National Institute of Advanced Industrial Science and Technology.

Senkovska, I., Hoffmann, F., Fröba, M., Getzschmann, J., Böhlmann, W., & Kaskel, S. (2009). New highly porous aluminium based metal-organic frameworks: Al(OH) (ndc) (ndc = 2,6-naphthalene dicarboxylate) and Al(OH)(bpdc) (bpdc = 4,4′-biphenyl dicarboxylate). *Microporous and Mesoporous Materials, 122*(1–3), 93–98. https://doi.org/10.1016/j.micromeso.2009.02.020

Sierra-Serrano, B., Garcia-Garcia, A., Hidalgo, T., Ruiz-Camino, D., Rodriguez-Dieguez, A., Amariei, G., … Rojas, S. (2022). Copper glufosinate-based metal-organic framework as a novel multifunctional agrochemical. *ACS Applied Materials & Interfaces, 14*(30), 34955–34962. https://doi.org/10.1021/acsami.2c07113

Singh, N., Qutub, S., & Khashab, N. M. (2021). Biocompatibility and biodegradability of metal organic frameworks for biomedical applications. *Journal of Materials Chemistry B, 9*(30), 5925–5934. https://doi.org/10.1039/d1tb01044a

Steenhaut, T., Filinchuk, Y., & Hermans, S. (2021). Aluminium-based MIL-100(Al) and MIL-101(Al) metal–organic frameworks, derivative materials and composites: Synthesis, structure, properties and applications. *Journal of Materials Chemistry A, 9* (38), 21483–21509. https://doi.org/10.1039/d1ta04444c

Su, S. K., & Wiley, R. C. (1998). Changes in apple juice flavor compounds during processing. *Journal of Food Science, 63*(4), 688–691. https://doi.org/10.1111/j.1365-2621.1998.tb15813.x

Terefe, N. S., Delon, A., Buckow, R., & Versteeg, C. (2015). Blueberry polyphenol oxidase: Characterization and the kinetics of thermal and high pressure activation and inactivation. *Food Chemistry, 188*, 193–200. https://doi.org/10.1016/j.foodchem.2015.04.040

Thommes, M., Kaneko, K., Neimark, A. V., Olivier, J. P., Rodriguez-Reinoso, F., Rouquerol, J., & Sing, K. S. W. (2015). Physisorption of gases, with special reference to the evaluation of surface area and pore size distribution (IUPAC Technical Report). *Pure and Applied Chemistry, 87*(9–10), 1051–1069. https://doi.org/10.1515/pac-2014-1117

Walker, J. M. (2009). *The protein protocols handbook* ((3rd ed.)). New York, N.Y.: Humana Press.

Wiśniewska, P., Haponiuk, J., Saeb, M. R., Rabiee, N., & Bencherif, S. A. (2023). Mitigating metal-organic framework (MOF) toxicity for biomedical applications. *Chemical Engineering Journal, 471*. https://doi.org/10.1016/j.cej.2023.144400

Wu, K., Du, C., Ma, F., Shen, Y., & Zhou, J. (2019). Optimization of metal-organic (citric acid) frameworks for controlled release of nutrients. *RSC Advances, 9*(55), 32270–32277. https://doi.org/10.1039/c9ra06939a

Xu, C., Cao, L., Liu, T., Chen, H., & Li, Y. (2023). pH-responsive copper-doped ZIF-8 MOF nanoparticles for enhancing the delivery and translocation of pesticides in wheat plants. *Environmental Science: Nano, 10*(9), 2578–2590. https://doi.org/10.1039/d3en00300k

Yoruk, R., & Marshall, M. R. (2003). Physicochemical properties and function of plant polyphenol oxidase: A review1. *Journal of Food Biochemistry, 27*(5), 361–422. https://doi.org/10.1111/j.1745-4514.2003.tb00289.x

Zhang, Q., Yang, H., Zhou, T., Chen, X., Li, W., & Pang, H. (2022). Metal-organic frameworks and their composites for environmental applications. *Advanced Science (Weinh), 9*(32), Article e2204141. https://doi.org/10.1002/advs.202204141